Modelling of submerged oscillating water columns with mass transfer for wave energy extraction

De Rooij, Sjors; Laguna, Antonio Jarquin

DOI
10.1109/OSES.2019.8867314

Publication date
2019

Document Version
Accepted author manuscript

Published in
Proceedings Offshore Energy and Storage Summit (OSES 2019)

Modeling of submerged oscillating water columns with mass transfer for wave energy extraction

Sjors de Rooij
dept. Hydraulic engineering
sect. Offshore and Dredging Engineering
Delft University of Technology
Delft, The Netherlands
S.P.A.derooij@student.tudelft.nl

Antonio Jarquin Laguna
dept. Marine and Transport Technology
sect. Offshore and Dredging Engineering
Delft University of Technology
Delft, The Netherlands
a.jarquinlaguna@tudelft.nl

***Abstract*—Oscillating-water-column (OWC) devices are a very important type of wave energy converters which have been extensively studied over the years. Although most designs of OWC are based on floating or fixed structures exposed above the surface level, little is known from completely submerged systems which can benefit from reduced environmental loads and a simplified structural design. The submerged type of resonant duct consists of two OWCs separated by a weir and air chamber instead of the commonly used single column. Under conditions close to resonance, water flows from the first column into the second one, resulting in a positive flow through the system from which energy can be extracted by a hydro turbine. While existing work has looked at the study of the behaviour of one OWC, this paper addresses the dynamic interaction between the two water columns including the mass transfer mechanism as well as the associated change of momentum. A numerical time-domain model is used to obtain some initial results on the performance and response of the system for different design parameters. The model is derived from 1D conservation of mass and momentum equations, including hydrodynamic effects, adiabatic air compressibility and turbine induced damping. Preliminary results indicate that the mass transfer has an important effect both on the resonance amplification and on the phase between the motion of the two columns. Simulation results are presented for the system performance over several weir heights and regular wave conditions. Further work will continue in design optimization and experimental validation of the proposed model.**

***Index Terms*—wave energy converter, submerged oscillating water column, mass transfer**

I. Introduction

In the past decades the demand and use of energy has increased, the majority of the energy is being generated by non-renewable energy resources. The finite supply and the significant environmental impacts of these energy sources has let to the increased demand for technologies exploding renewable energy. The potential global wave power resource is estimated around 2TW [1], harvesting energy from waves is a promising resource. Over the years many types of wave energy converters (WEC) have been developed [2]. The work of this paper is based on the oscillating-water-column (OWC) type of WEC. The basic geometrical configuration of an OWC comprises a large chamber inside a floating or fixed structure connected to the open sea via an opening in the vertical wall. Inside the chamber fluctuation of the water column elevation compresses and expands the air, forcing it in and out the chamber through a turbine to the atmosphere. The OWC's dynamics and energy conversion mechanism have been extensively investigated and a number of OWCs have been built and tested. Since the 80s various OWC plants have been operative [3].

Although extensive research has been done on this basic configuration little is known about completely submerged systems using oscillating water columns. The submerged resonant duct, analysed in this paper was proposed by D. Carey in the late 70s [4] and consists of two water columns separated by a weir and an air chamber. Under resonance conditions water flows over the weir into the second column, resulting in a positive mean flow through the full system. The hydraulic turbine placed at the exit of the second column extracts the kinetic energy contained in the flow. Previous work has elaborated on the behaviour of a single submerged column [5]–[10] excluding the interaction between the two columns and the turbine. Additionally in these and other works [11]–[13] the time dependent Bernoulli equation has been used as basis for the equation of motion, neglecting the momentum associated by the change of mass. This paper addresses the dynamic non-linear interaction of the coupled water column, including the mass transfer [10] and its associated change of momentum. Furthermore, the behaviour of the turbine is included in the time-domain analysis of the system.

II. Time-domain numerical model

A. System description

Consider the submerged OWC shown in Fig. 1. The OWC consist of an air chamber with initial volume V_0 and the initial pressure p_0 corresponding to the atmospheric p_{atm} and hydrostatic pressure $\rho g h_c$ in equilibrium position at depth h_c. The level of the weir, separating the two water columns, z_w is measured in upward direction from depth h_c. The two columns are denoted by subscripts 1 and 2, the areas of the column A_1, A_{c1} and A_{c2} are assumed constant along the streamlines L_1, L_{c1} and L_{c2}. The area of the exit duct along streamline L_1 is a function of the turbine diameter $A_2 = \frac{1}{4}\pi D_t^2$. The in-plane width of the structure is denoted by L_t. Lastly the horizontal

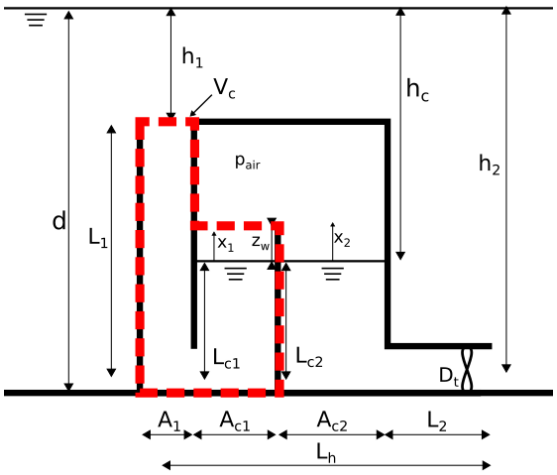

Fig. 1. Cross-section of the submerged Oscillating water column, symbols denote geometrical characteristics.

distance between the center of the mouth of the first column to the exit of the second column is denoted by L_h

B. Motion of the water column

The equation of motion of a submerged water column is derived using the control volume V_c indicated by the dashed red box in Fig. 1 , the full length of the volume is from the entrance to the weir level with variable cross section A_{c1} and A_1. For free-surface levels of $x_1 < z_w$ the volume is only partially filled, resulting in the mass changes related with the surface level of the columns. The equations of motion including this change of mass are derived from the equations of conservation of momentum and mass. The momentum equation is given by [14]:

$$\begin{aligned}\int_{V_c} \frac{\partial \rho \mathbf{v}}{\partial t} + \nabla \cdot (\rho \mathbf{v}\mathbf{v}) \; dV_c &= \int_S -p\mathbf{n} \; dS + \int_{V_c} \rho \mathbf{g} \; dV_c \\ &= \int_{V_c} -\nabla p + \rho \mathbf{g} \; dV_c\end{aligned} \tag{1}$$

Where g is the gravitational acceleration, ρ the water density, $\mathbf{v}$ the local velocities and p the external pressures. Equation (1) holds for any control volume, thus the integrands vanishes from the equation:

$$\frac{\partial \rho \mathbf{v}}{\partial t} + \nabla \cdot (\rho \mathbf{v}\mathbf{v}) = -\nabla p + \rho \mathbf{g} \tag{2}$$

Rewriting the second term in (2) by:

$$\nabla \cdot (\rho \mathbf{v}\mathbf{v}) = [\nabla \cdot (\rho \mathbf{v})]\mathbf{v} + \rho \mathbf{v} \cdot \nabla \mathbf{v} \tag{3}$$

and applying the chain rule differentiation results in the conservation of momentum equation from which the forces associated by the change of mass times the velocity, the acceleration and the external pressure can be distinguished:

$$\left[\frac{\partial \rho}{\partial t} + \nabla \cdot (\rho \mathbf{v})\right] \mathbf{v} + \rho \left[\frac{\partial \mathbf{v}}{\partial t} + \mathbf{v} \cdot \nabla \mathbf{v}\right] = -\nabla p + \rho \mathbf{g} \tag{4}$$

The expression for the change of mass can be derived from the conservation of mass equation [14]. Assuming a rigid body translation of the fluids the displacement and the associated change of mass can both be expressed as a function of the flow velocity.

$$\int_V \frac{\partial \rho}{\partial t} dV + \int_V \nabla \cdot (\rho \mathbf{v}) \, dV = \rho A_{c1} \dot{x}_1 \tag{5}$$

Solving the integrands for the control volume $V_c = L_1 A_1 + (L_{c1} + z_w) A_{c1}$ results in the following expression for the change of mass:

$$\left[\frac{\partial \rho}{\partial t} + \nabla \cdot (\rho \mathbf{v})\right] = \frac{\rho A_{c1} \dot{x}_1}{V_c} \tag{6}$$

Further, by assuming an inviscid and irrotational fluid with a constant density the acceleration term in (4) can be simplified to:

$$\rho \left[\frac{\partial \mathbf{v}}{\partial t} + \mathbf{v} \cdot \nabla \mathbf{v}\right] = \rho \frac{\partial \mathbf{v}}{\partial t} + \rho \nabla \frac{1}{2} \mathbf{v}^2 \tag{7}$$

Substituting both expressions of (6) and (7) in (4) and integrating over the streamline results in the equation of motion of the column expressed in pressure.

$$\begin{aligned}\rho(\frac{A_{c1}}{A_1} L_1 + L_{c1} + x_1)\ddot{x}_1 + \frac{A_{c1} x_1}{V_c} \rho \dot{x}_1^2 + \rho \frac{\dot{x}_1^2}{2} \\ = p - \rho g x_1\end{aligned} \tag{8}$$

C. Weir Discharge

Equation (8) describes the motion behaviour of $x_{1,2} < z_w$. When the displacement exceeds the weir level water is discharged to the other column and requires the equation to be modified. The fluid is assumed to be drawn off instantaneously, the discharge is denoted by Q_w and positive for flow from column 1 to column 2. The value weir discharge, for the displacements and velocities conditions presented in Fig. 2 is given by:

$$Q_w = \begin{array}{cl} \dot{x}_1 A_{c1} & x_1 \geq z_w \; , \; x_2 < z_w \; , \; \dot{x}_1 > 0 \\ (\dot{x}_1 - \frac{\dot{x}_1 A_{c1} + \dot{x}_2 A_{c2}}{A_{c1} + A_{c2}}) A_{c1} & x_1 \geq z_w \; , \; x_2 \geq z_w \\ -\dot{x}_2 A_{c2} & x_1 < z_w \; , \; x_2 \geq z_w \; , \; \dot{x}_2 > 0 \\ 0 & x_1 < z_w \; , \; x_2 < z_w \end{array} \tag{9}$$

Introducing the weir discharge decouples the free-surface elevation from the velocity of the column, the free-surface is now described by:

$$\begin{aligned} x_1 &= \int_{t_0}^{t} \left(\dot{x}_1 - \frac{Q_w}{A_{c1}}\right) dt \\ x_2 &= \int_{t_0}^{t} \left(\dot{x}_2 + \frac{Q_w}{A_{c2}}\right) dt \end{aligned} \tag{10}$$

With the fluid being drawn the velocity and momentum at the free surface is decreased, resulting in the expressions for the convective and mass change momentum of:

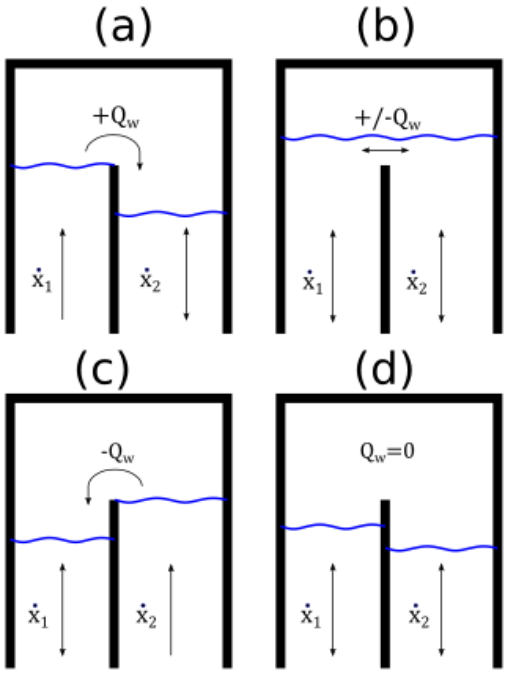

Fig. 2. Weir discharge for displacement and velocity conditions. (a) for $x_1 \geq z_w$ and $\dot{x}_1 \geq 0$ while $x_2 \leq z_w$ and for all values of $\dot{x}_2$, (b) for $x_{1,2} \geq z_w$ for all values of $\dot{x}_{1,2}$, (c) for $x_2 \geq z_w$ and $\dot{x}_2 \geq 0$ while $x_1 \leq z_w$ and for all values of $\dot{x}_1$, (d) for $x_{1,2} \leq z_w$ and all values of $\dot{x}_{1,2}$

$$\begin{aligned} \rho\frac{\dot{x}_1^2}{2} &= \rho\frac{(\dot{x}_1 - \frac{Q_w}{A_{c1}})^2}{2} \\ \rho\frac{\dot{x}_2^2}{2} &= \rho\frac{(\dot{x}_2 + \frac{Q_w}{A_{c2}})^2}{2} \end{aligned} \tag{11}$$

$$\begin{aligned} \frac{A_{c1}x_1}{V_c}\rho\dot{x}_1^2 &= \frac{A_{c1}x_1}{V_c}\rho\left(\dot{x}_1 - \frac{Q_w}{A_{c1}}\right)^2 \\ \frac{A_{c2}x_2}{V_c}\rho\dot{x}_2^2 &= \frac{A_{c2}x_2}{V_c}\rho\left(\dot{x}_2 + \frac{Q_w}{A_{c2}}\right)^2 \end{aligned} \tag{12}$$

Additionally, the drop of water from the weir on the free surface of the column gives an additional impact pressure. The magnitude of the impulse is determined assuming the instantaneous discharge and mass transfer. The velocity of the dropping water is derived from the potential and kinetic energy relation depending on the difference between the weir level and the column displacement.

$$\rho g(z_w - x) = \frac{1}{2}\rho v_{drop}^2 \tag{13}$$

The impact force is calculated from the velocity difference of the dropping water and the column and the weir discharge, resulting in an impact pressure of:

$$p_{drop,2} = \begin{matrix} \frac{(v_{\text{drop},2}+\dot{x}_2)\rho|Q_w|}{A_{c2}} & x_1 \geq z_w,\ x_2 < z_w \\ 0 & x_1 > z_w \end{matrix} \tag{14}$$

$$p_{drop,1} = \begin{matrix} \frac{(v_{\text{drop},1}+\dot{x}_1)\rho|Q_w|}{A_{c1}} & x_2 \geq z_w,\ x_1 < z_w \\ 0 & x_2 > z_w \end{matrix} \tag{15}$$

It is important to mentions that the impact is assumed to be spread over the full area of the second column. In reality the drop acts locally and will affect the internal free-surface variations.

D. Air chamber dynamics

Apart from the mass transfer the columns are coupled by the pressure in the air chamber. The mass of air in the air chamber is $M = \rho_{air}(t)V(t)$, being $\rho_{air}(t)$ the air density and $V(t)$ the air volume. The air volume is given by the equation:

$$V(t) = V_0 - A_{c1}x_1 - A_{c2}x_2 \tag{16}$$

Given the small temperature oscillations and short timescale for heat exchange, the thermodynamic process is assumed both adiabatic and reversible. The equation of the relation between the air density and the air pressure for this isentropic process is:

$$\left(\frac{p_0}{p_{(a)}}\right)^{\frac{1}{\gamma}} = \left(\frac{\rho_0}{\rho(t)}\right) \tag{17}$$

where ρ_0 is the initial air density and γ the polytropic exponent, here a value of $\gamma = 1.4$ is used for the isentropic process. Assuming little air is discharged inside the water, the continuity of mass holds:

$$\frac{d\rho(t)V(t)}{dt} = \dot{\rho}(t)V(t) + \dot{V}(t)\rho(t) = 0 \tag{18}$$

Substituting (16) and (17) into (18) gives the equation that describes the dynamics of the air chamber.

$$\dot{p}_{air} = \gamma\frac{A_{c1}\dot{x}_1 + A_{c2}\dot{x}_2}{V_0 - A_{c1}x_1 - A_{c2}x_2}(p_0 + p_{air}) \tag{19}$$

E. Turbine pressure

A hydraulic turbine is used to extract the energy from the constrained flow in the second column. In the proposed model, the operating turbine is introduced as a reaction pressure on the equation of motion of the water column.

The turbines pressure p_{tur} is obtained from the power generated by the turbine P_{tur} as a function of its specific speed and unit discharge through the turbine. For bulb turbines this relation is obtained from empirical regression relations found in [15]:

$$P_{tur} = \left(390.591\left(\frac{Q(t)}{D_t^2 H(t)^{0.5}}\right)^{0.8209}\frac{H(t)^{1.25}}{N}\right)^2 \tag{20}$$

$$p_{tur} = \frac{P_{tur}}{Q(t)} \tag{21}$$

Where N is the rotation speed of the turbine in rpm, $H(t)$ is the dynamic head of the flow through the turbine in meters, and $Q(t)$ is the flow discharge in cubic meters per second:

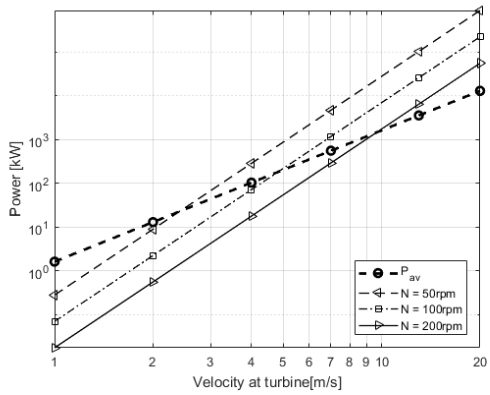

Fig. 3. Relation between turbine power output and available power P_{av} versus the fluid velocity at the turbine for different rotational speeds according to empirical relations from Bulb turbines [16]; a turbine diameter of 2m is used.

$$H(t) = \frac{\frac{1}{2}\rho\left(\frac{A_{c2}}{A_2}\dot{x}_2\right)^2}{\rho g} \tag{22}$$

$$Q(t) = A_{c2}\dot{x}_2 \tag{23}$$

The empirical relation in (20) was obtained from operating turbines under stationary pressure and discharge conditions and is does not include any dynamic effects which might could be derived from oscillatory flows and pressures. For the current application this assumption implies instantaneous changes in the turbine reaction and extracted power which become more relevant for larger systems, nevertheless this simplified model gives sufficient insight for the purpose of this work on the coupling effect that the turbine pressure has on the motion of the water flow. For this paper, energy extraction from the turbine is only considered for the flow exiting the system (unidirectional flow), when the flow is in the opposite direction, the flow is assumed to be undisturbed by the presence of the turbine, i.e. the pressure reaction from the turbine is zero when flow is coming from the exit opening.

In Fig. 3 the performance curve of the turbine is given for different velocities with a turbine diameter $D_t = 2m$. The available power P_{av} in the flow is calculated from the dynamic pressure and discharge at the turbine:

$$P_{av} = \left(\frac{1}{2}\rho\left(\frac{A_{c2}}{A_2}\dot{x}_2\right)^2\right)\cdot(A_{c2}\dot{x}_2) \tag{24}$$

Is it observed in Fig. 3, that for a constant rotational speed the output power demanded by the turbine can be higher than the available power in the flow. In this case a turbine with variable speed operation would be able to deal with this difference. In this paper, the results with velocities higher than the limit velocity will be used to determine the power potential of the device.

F. Wave pressure

The pressure variation at the opening is derived from linear wave theory, simplified by assuming a undisturbed wave field over the fully submerged structure. Additionally, a uniform pressure at the opening is assumed under the condition of the wave length being much longer compared to the width of the opening. The equation for the excitation pressure caused by a regular wave on both columns is:

$$p_{w,1} = \rho g a \frac{cosh(k(-h_1+d))}{cosh(kd)} sin(\omega_w t - 0) \tag{25}$$

$$p_{w,2} = \rho g a \frac{cosh(k(-h_2+d))}{cosh(kd)} sin(\omega_w t - kL_h) \tag{26}$$

Where, a is the wave amplitude, k is the wave number, ω_w the wave frequency and b_2 the horizontal distance between openings of column 1 and column 2.

G. Radiation pressure

The hydrodynamic end-effects are determined from [5]. Here the pressures related to the added mass p_a and radiation damping p_r are a function of the wave length L_w, depth of the entrance h, the width $b = \frac{A}{L_t}$ and respectively the acceleration and velocity of the column. In this paper response is analysed for regular waves only, simplifying the equations for the pressure of the added mass and radiation damping in the time domain to:

$$p_a = \rho L_a(L_w, h, b)\frac{A_c}{A}\ddot{x} \tag{27}$$

$$p_r = \rho\omega_w D_r\left(L_w, h, b\right) b\dot{x} \tag{28}$$

Where L_a is the added length and D_r the radiation damping coefficient.

The dimensions of the model are tuned for a resonance at wave periods around 8.5 seconds in first column and a no resonance in the second column due to the difference in inertia. Additionally the dimensions of the second column are outside the range of the radiation coefficients in [5]. Therefore the radiation forces are applied to the first column only, in the second column the radiation damping is introduced as a pressure loss at the exit. The added length $L_{a,2}$ is incorporated in the equivalent length of the second column.

$$L_{eq,2} = L_2 + L_{a,2} \tag{29}$$

H. Pressure losses

In the calculation the pressure losses in the first column are assumed

$$p_{loss} = \frac{1}{2}K_w\left(\frac{A_c}{A}\right)^2\dot{x}\,|\dot{x}| \tag{30}$$

Where the value of $K_{w,1} = 0.75$ is used for the U-shaped vertical duct [11]. A value of $K_{w,2} = 0.75$ is assumed for the pressure losses in the second column, related to the velocity at the exit [17].

I. Overall system equations

Here the overall system, shown in Fig. 1, is considered. Combining all external pressures in (8) give the following equations of motion of the two columns, together with (19) these are the three differential equations describing the behaviour of the system.

$$\begin{aligned}\rho(\frac{A_{c1}}{A_1}L_1 + L_{c1} + x_1)\ddot{x}_1 + \rho\frac{\left(\dot{x}_1 - \frac{Q_w}{A_{c1}}\right)^2}{2} \\ + \frac{A_{c1}x_1}{V_{c1}}\rho\left(\dot{x}_1 - \frac{Q_w}{A_{c1}}\right)^2 + \rho g x_1 + p_{air} \\ = p_{w,1} + p_{r,1} + p_{a,1} - p_{loss,1}\end{aligned} \tag{31}$$

$$\begin{aligned}\rho\left(L_{c2} + x_2 + \frac{A_{c2}}{A_2}L_{eq,2}\right)\ddot{x}_2 + \rho\frac{\left(\dot{x}_2 + \frac{Q_w}{A_{c2}}\right)^2}{2} \\ + \frac{A_{c2}x_2}{V_{c2}}\rho\left(\dot{x}_2 + \frac{Q_w}{A_{c2}}\right)^2 + \rho g x_2 + p_{air} \\ = p_{w,2} + p_{tur,2} - p_{loss,2}\end{aligned} \tag{32}$$

III. Results and discussion

The present model is used to simulate the performance and analyse the influence of the mass transfer between columns. The dimensions given in Table I are determined for a resonance to regular waves with a period of 8.5 seconds.

TABLE I
DIMENSIONS

Variable	unit	value
d	m	40
h_1	m	20
h_2	m	39
h_c	m	30
p_{atm}	Pa	1.01e5
γ	$-$	1.4
ρ_w	kgm^{-3}	1025
g	ms^{-2}	9.811
L_{c1}	m	10
L_1	m	20
L_{c2}	m	10
$L_{eq,2}$	m	15.5
A_{c1}	m^2	40
A_{c2}	m^2	160
A_1	m^2	28.5
D_t	m	2
A_2	m^2	3.14
V_0	m^3	2000

A. Dynamic response without turbine

The submerged-OWC response is obtained in the time domain by solving numerically the differential equations presented in the last section. The commercial software Matlab was used to perform the numerical integration via the ODE45 variable time step solver. Zero initial conditions were used.

The outputs are the displacements of the inner free surfaces x_1 and x_2, the flow velocities of the column $\dot{x}_1$ and $\dot{x}_2$ in cross sections A_{c1} and A_{c2} and the air pressure difference p_{air} corresponding to the time domain vector t. The post-processing of the output involves the computation of the power output and average and maximum values of the variables. This is performed on the last five periods of the response to obtain the steady state response.

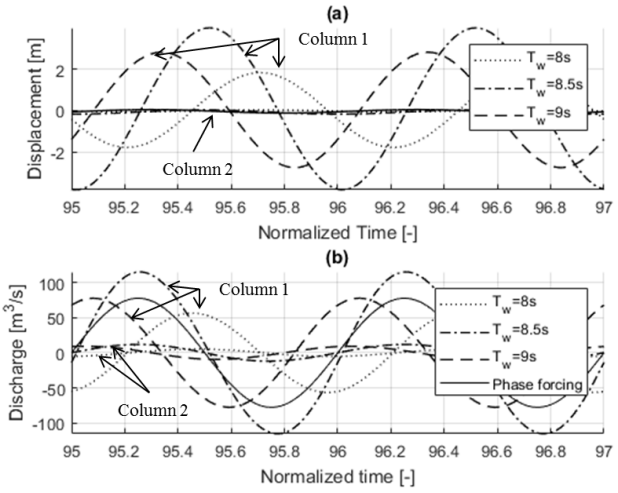

Fig. 4. Time domain response column 1 and 2 excluding mass transfer through weir discharge, (a): Displacement, (b): Discharge.

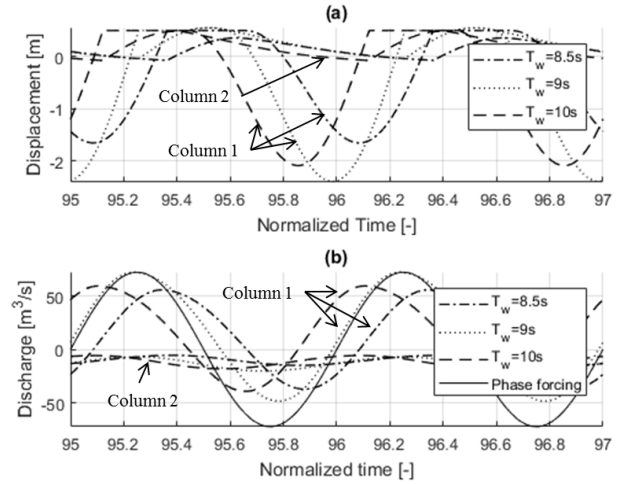

Fig. 5. Time domain response column 1 and 2 including weir discharge for a weir level of $z_w = 0.5m$, (a): Displacement, (b): Discharge.

The time domain results for a response excluding a weir discharge is presented in Fig. 4 and in Fig. 5 the response is given for a weir level with the value $z_w = 0.5m$. In both figures the response is obtained for regular waves with amplitude $a_w = 2m$ and different wave periods. The time axis is normalized by the excitation period of each response $\tilde{t} = \frac{t}{T_w}$.

In Fig. 6, 7, 8 and 9 the maximum and mean values of the displacement and discharge of both columns are presented for different weir levels and regular waves with amplitude $a_w =$

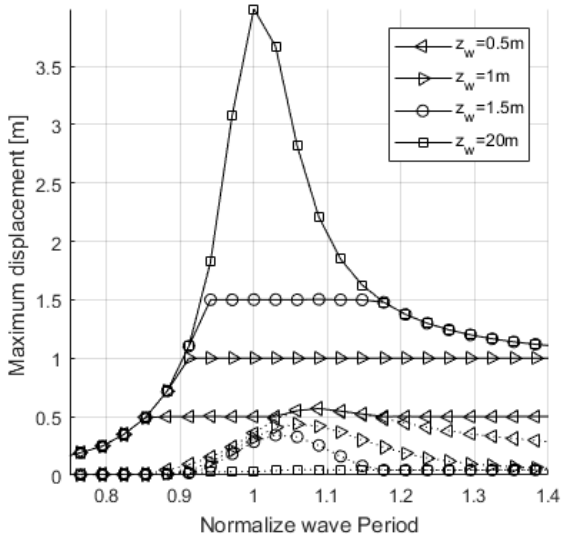

Fig. 6. Maximum displacement for different weir levels excluding power take-off. Continuous lines: response of the first column. Dashed lines: response of the second column

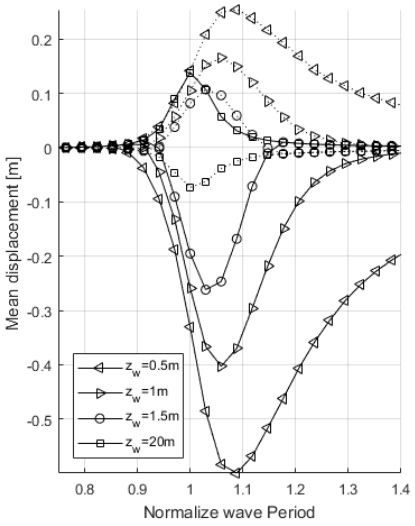

Fig. 8. Mean displacement for different weir levels excluding power take-off. Continuous lines: response of the first column. Dotted lines: response of the second column

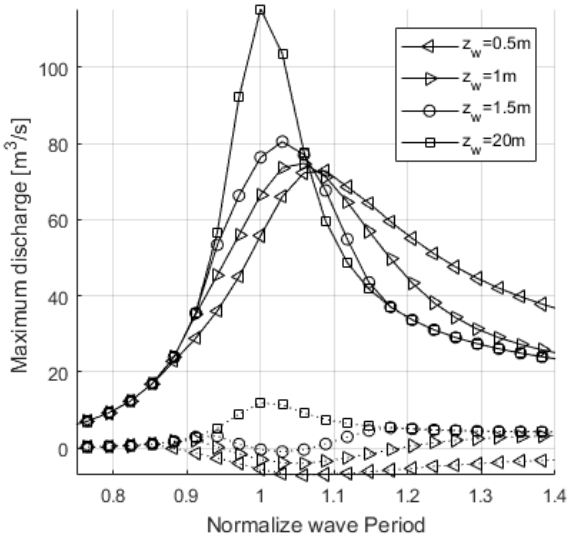

Fig. 7. Maximum discharge for different weir levels excluding power take-off. Continuous lines: response of the first column. Dashed lines: response of the second column

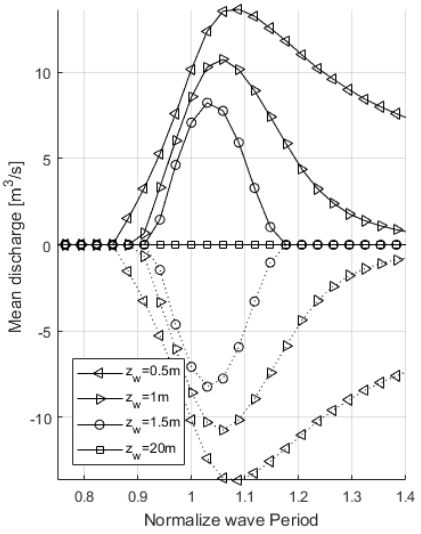

Fig. 9. Mean discharge for different weir levels excluding power take-off. Continuous lines: response of the first column. Dotted lines: response of the second column

$2m$. The time axis is normalized with respect to the design period of the system $T_n = 8.5s$.

From the results certain features are evident: firstly, a clear relation between a low weir level and a high discharge is observed. The high discharge results in a negative maximum discharge in the second column, indicating a uni-directional flow in the direction of the exit. Related to the discharge, a shifts in the period of the maximum response amplitude is observed. For a weir level of $z_w = 0.5m$ with a high discharge the resonance occurs at a period approximately 10 % higher than the design period. In [10] a period shift of 25 % was observed for a single column water column subjected to atmospheric pressures at the free surface. The difference can be explained by the difference in restoring force in both models. In the present model the restoring force is composed of the gravitational force and the air pressure. The gravitational restoring force is decreased by the weir discharge, but on the other hand the volume of air remains the same and thus the restoring force of the air pressure is unchanged. The relative reduction in the restoring force and thus stiffness is lower compared to the experiment results presented in [10], resulting in smaller shifts in natural periods. In Fig. 5 (b) the effect

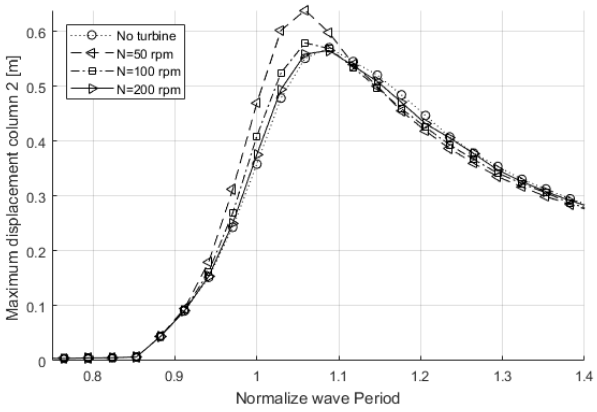

Fig. 10. Maximum displacement of the second column against the periods of regular waves with amplitude $a_w = 2m$ for $z_w = 0.5m$ including the turbine response

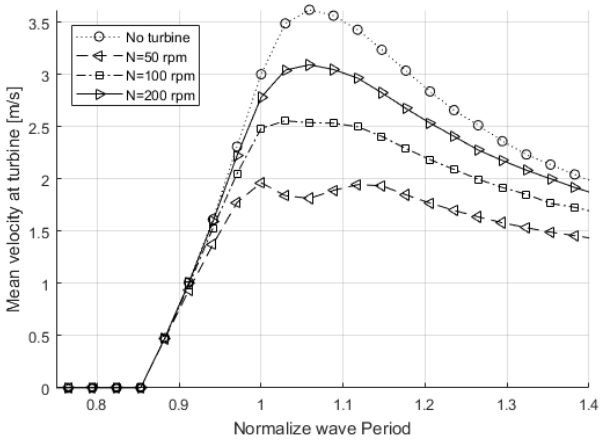

Fig. 11. Mean velocity at the turbine against the periods of regular waves with amplitude $a_w = 2m$ for $z_w = 0.5m$ including the turbine response

of the reduced restoring force can be seen, here the troughs of the discharge oscillations are shifted to a later moment in time with respect to the oscillation of the force compared to its maximum amplitude. In Fig. 4 (b the maximum and minimum amplitude of the discharge is fully in phase with the forcing with a wave period of 8.5 seconds, indicating resonance conditions as expected for the given design period. Furthermore, a change in mean displacement is observed in both columns, a decrease in the first and an increase in the second column. This is a result of the high velocities and damping in the second column. Higher velocities, thus discharges, in the second column result in a higher resistance of the flow increasing the mean displacement of the second column. Consequently, the mean displacement in the first column is reduced by the coupling with the air pressure. The change in mean displacement also reduces the potential weir discharge. In a model without head losses in the second column a smaller change in mean displacements was found, including a higher discharge.

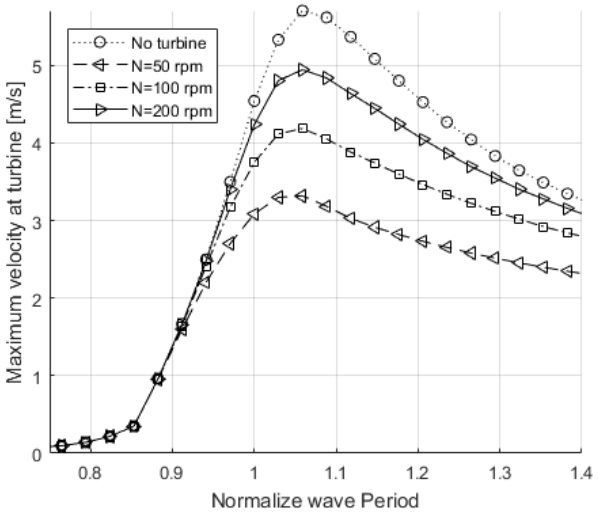

Fig. 12. Maximum velocity at the turbine against the periods of regular waves with amplitude $a_w = 2m$ for $z_w = 0.5m$ including the turbine response

B. Dynamic response including turbine

Next, the dynamic response of the presented model is derived including energy extraction by the turbine. The results are again computed for regular waves with amplitude $a_w = 2m$ and different periods. The results for the modelled turbines with constant speeds $N = 50, 100$ and 200 rpm and for a weir level of $z_w = 0.5m$ are compared to the results without the turbine. The presented results are for the second column only.

In Fig. 10 the maximum displacement of the second column is presented. In Fig. 11,12 and 13 the mean, maximum and minimum velocities at the turbine are presented. Lastly, the mean generated power is given in Fig. 14.

The first clear distinction seen in the figures is the relation between a high power generation and the lower velocities of the second column caused by the decrease and increase of the mean displacements in respectively column 1 and 2, which was also observed in the previous section. Furthermore, from the graphs two effects of the decreased discharge can be seen. Firstly, the maximum response amplitude moves toward the design natural period of the model. Secondly, the maximum amplitude in the maximum and mean velocity is becoming flatter for an increased power generation. The amplitude of the oscillations remain approximately the same a the same wave period for the different rotations speeds, this results in a reversed shape in the amplitude of the minimum velocity response at the resonance period. To avoid stall of the turbine reversed flow through the turbine is not desirable, therefore an optimal value should be found in the power generation and the dynamic response. For the optimization it is important to note that the maximum velocities of the $N = 50$ rpm are higher than the limit velocity found in Fig. 3. Despite the overestimation of the generated power with respect to the

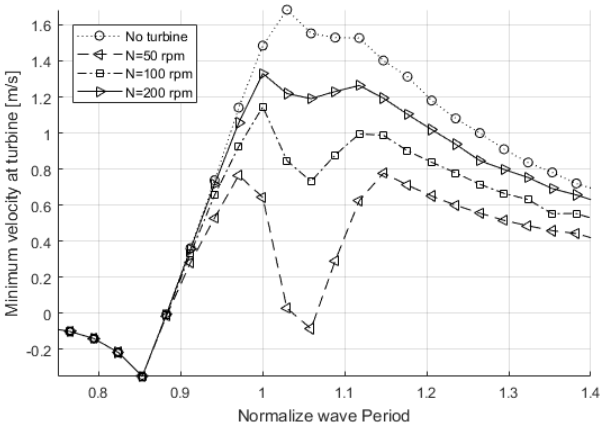

Fig. 13. Minimum velocity at the turbine against the periods of regular waves with amplitude $a_w = 2m$ for $z_w = 0.5m$ including the turbine response

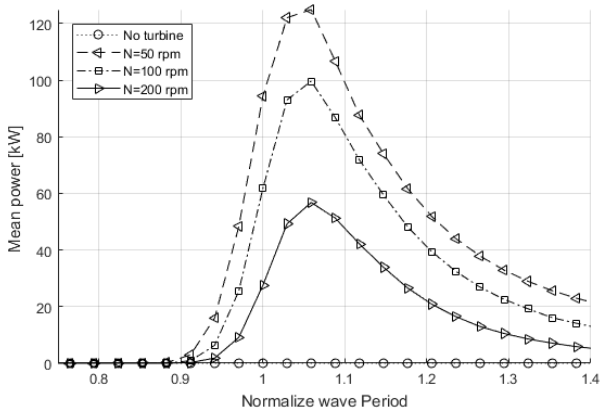

Fig. 14. Mean generated power against the periods of regular waves with amplitude $a_w = 2m$ for $z_w = 0.5m$ including the turbine response

extraction capacity of the turbine at this speed, the response is not critically damped and the flow at the turbine remained unidirectional. Therefore the optimal power generation is assumed to lay close to the power value found for a rotation speed of $N = 50$ rpm. A turbine with variable rotational speed needs to be designed to be able to extract the available power. Such turbine should be able to react to the velocity oscillations in a relatively shorter period when compared to conventional hydraulic turbines.

A capture width ratio between the 7.5 and 12 % was found, comparing the captured energy to the available energy in regular waves in intermediate depths [18]. This research was focused on the effect of the mass transfer of the system. Additional optimizations regarding the energy transfer between the columns and in the turbine are expected to increase its efficiency.

IV. Conclusion and recommendations

This paper presented the analysis of the behaviour of a wave energy converter. The WEC consists of two columns subject to air pressure and mass transfer between the columns The time-domain response was obtained by solving numerically the differential equations used to model the device under the excitation of regular waves. The model was derived from physical principles which include the instantaneous mass transfer, the isentropic process for expansion and compression of air, the response of a hydraulic turbine and hydrodynamic pressure using the potential wave theory. The effect of pressure losses caused by friction, turbulence, viscosity and vortex shedding at the entrances are taken into account in the form of a pressure loss coefficient. The results show that the mass transfer reduces the gravitational restoring force in the discharging column, while the receiving column gains mass and thus potential energy together. Furthermore, the free-surface elevation is decoupled from the discharge inside the water column, having a direct effect on the pressures at the free surface related to the convective acceleration and the change of mass. The falling water generated an impact force on the receiving column which should not be neglected in the analysis. A shift in resonance periods is observed in the results, depending on the magnitude of weir discharge an increase up to 10% of the design periods was identified. This shift can contribute to broaden the bandwidth of the resonance periods to optimize the dynamic behaviour. The model provides a useful insight on the behaviour of submerged oscillating water columns and the results can provide a basis for design optimizations. Future work includes experimental validation and evaluation of a control strategy with respect to the operation of the turbine subject to oscillatory flows.

V. Acknowledgment

This work was caried out during the MSc graduation project at Delft University of Technology for the section Offshore and Dredging Engineering. The authors would like to thank the members of Neptune Energy LTD, A. Göbel and F. Gerner for the opportunity to work on this concept.

References

[1] G. Mørk, S. Barstow, A. Kabuth, and M. T. Pontes, "Assessing the global wave energy potential," in *Proceedings of International Conference on Ocean, Offshore Mechanics and Arctic Engineering*, no. 29, (Shanghai), pp. 1–8, ASME, 2010.

[2] L. Rusu and F. Onea, "The performance of some state-of-the-art wave energy converters in locations with the worldwide highest wave power," *Renewable and Sustainable Energy Reviews*, vol. 75, no. November 2016, pp. 1348–1362, 2017.

[3] A. F. Falcão and J. C. Henriques, "Oscillating-water-column wave energy converters and air turbines: A review," *Renewable Energy*, vol. 85, pp. 1391–1424, 2016.

[4] D. J. Carey and Z. Meratla, "Apparatus for converting wave energy into electricity," 1976.

[5] J. Lighthill, "Two-dimensional analyses related to wave-energy extraction by submerged resonant ducts," *Journal of Fluid Mechanics*, vol. 91, no. 2, pp. 253–317, 1979.

[6] G. F. Knott and J. O. Flower, "Wave-tank experiments on an immersed parallel-plate duct," *Journal of Fluid Mechanics*, vol. 90, no. 2, pp. 327–336, 1979.

[7] G. F. Knott and J. O. Flower, "Measurement of energy losses in oscillatory flow through a pipe exit," *Applied Ocean Research*, vol. 2, no. 4, pp. 155–164, 1980.

[8] J. R. Thomas, "The absorption of wave energy by a three-dimensional submerged duct," *Journal of Fluid Mechanics*, vol. 104, pp. 189–215, 1981.
[9] M. J. Simon, "Wave-energy extraction by a submerged cylindrical resonant duct," *Journal of Fluid Mechanics*, vol. 104, no. 7, pp. 159–187, 1981.
[10] G. F. Knott and J. O. Flower, "Simulation studies of basic non-linear effects of wave-energy conversion by an overtopping water column," *Energy Conversion*, vol. 19, pp. 59–69, 1978.
[11] P. Boccotti, "On a new wave energy absorber," *Ocean Engineering*, vol. 30, no. 9, pp. 1191–1200, 2003.
[12] G. Malara and F. Arena, "Analytical modelling of an U-Oscillating Water Column and performance in random waves," *Renewable Energy*, vol. 60, pp. 116–126, 2013.
[13] S. Czitrom, R. Godoy, E. Prado, P. Pérez, and R. Peralta-Fabi, "Hydrodynamics of an oscillating water column seawater pump," *Ocean Engineering*, vol. 27, no. 11, pp. 1181–1198, 2000.
[14] P. Kundu and Cohen I.M., *Fluid Mechanic*. Elsevier, fourth edition ed., 1987.
[15] W. Knapp, C. Böhm, J. Keller, W. Rohne, and R. Schilling, "Turbine development for the Wave Dragon wave energy converter," tech. rep., Technische Universität München, München, 2003.
[16] C. Kpordze and C. Warnick, "Experience curves for modern low-head Hydroelecric turbines." 1983.
[17] A. Kotowski, H. Szewczyk, and W. Ciezak, "Entrance loss coefficients in pipe hydraulic systems," *Environment Protection Engineering*, vol. 37, no. 4, pp. 105–117, 2011.
[18] L. Holthuijsen, *Waves in oceanic and coastal waters*. Cambridge Uniersity Press, 2007.